AAS 12-202

RELATIVE NAVIGATION FOR SATELLITES IN CLOSE PROXIMITY USING ANGLES-ONLY OBSERVATIONS

Hemanshu Patel[1], T. Alan Lovell[2], Shawn Allgeier[3], Ryan Russell[4], Andrew Sinclair[5]

Relative navigation using angles-only observations is explored in this research. Previous work has shown that the unique relative orbit of a deputy satellite cannot be found using angles-only camera measurements from the chief satellite when a linear model of relative motion is used, due to a lack of observability. This work examines the possibility of partial observability, which in this case consists of a basis vector that corresponds to a family of relative orbits. An initial orbit determination (IOD) method is introduced that uses 3 Line-Of-Sight (LOS) measurements and provides an initial guess for the basis vector. This guess is differentially corrected with a batch estimator that takes in a full set of LOS measurements to hone in on a converged solution for the basis vector.

INTRODUCTION

In performing relative navigation (i.e. relative orbit determination) for satellites in close proximity, two observation sensors are typically used. These are cameras and range sensors on the satellites. The problem that is examined here is a case where the only observation tool is a camera. This means the only information available is the line-of-sight (LOS) unit vectors, which can be resolved into azimuth and elevation angles in a particular frame. Woffinden and Geller[1] stated that, due to lack of observability, the unique relative orbit cannot be found if the following three conditions are satisfied:

- only LOS measurements are taken (i.e. range between satellites is unavailable)
- a linear model of relative motion is used to estimate the dynamics
- there are no thrusting maneuvers during the span of measurements

[1] Aerospace Engineer, Emergent Space Technologies, Greenbelt, MD.
[2] Research Aerospace Engineer, Air Force Research Laboratory, Space Vehicles Directorate, Kirtland AFB, NM.
[3] Aerospace Engineer, Schafer Corporation, Albuquerque, NM.
[4] Assistant Professor, Department of Aerospace Engineering and Engineering Mechanics, The University of Texas at Austin, Austin, TX.
[5] Associate Professor, Department of Aerospace Engineering, Auburn University, Auburn, AL.

Strictly speaking, if any one of these restrictions is relaxed, all six relative states are observable. However, there may be significant uncertainty in the solution. Consider the case of processing range measurements along with the angle measurements. If range measurements are frequently available (comparable to the sample rate of the angle measurements), one would have a high degree of confidence in the solution. However, if range is only sparsely available (say, once or twice over the fit span), one's confidence level in the solution would be significantly lower, especially if there is substantial error in the range measurements.

The same is true for the case of a small number of maneuvers over the fit span. The effect of an impulsive maneuver is to change the relative motion profile; this change is a function of both the maneuver itself and the range between satellites at the time of the maneuver. As with the case of infrequently available range measurements, one's confidence level in the solution would be significantly lower for the case of sparse maneuvers than for frequent maneuvers, especially if there is substantial error in the maneuvers. Finally, even when using a nonlinear model to estimate the dynamics, close proximity causes the nonlinearities to be difficult to observe because the smaller the separation between the chief and deputy is, the more similar the linear and nonlinear models of the motion tend to look. Several researchers have investigated relaxing one or more of the three above restrictions and observed the resulting quality of the unique six-state solution[2-4]. Another researcher[5] used curvilinear rather than rectilinear coordinates to account for the curvilinear aspect of relative motion that is normally neglected when using a rectilinear frame. As with nonlinearities, these differences vanish for smaller separation between chief and deputy, again resulting in high uncertainty of the six-state solution.

Ref. 1 showed that a family of relative orbits whose state histories are proportional to one another (i.e. differ by only a constant scalar multiple) will possess a common LOS history. Figure 1 shows what is meant by a family of relative orbits. The statement of Ref. 1 implies that in cases where the unique relative trajectory cannot be determined, it should be possible to determine a basis vector for the family on which that trajectory resides. So, just as with angles-only navigation where the direction of the position vector between the satellites is known but its magnitude cannot be determined, the same is true for this basis vector: its direction (in six-dimensional space) is known but its magnitude cannot be determined.

The goal of this paper is to develop a technique for determining the basis vector of a relative trajectory (i.e., only five elements of the six-state vector) given angles-only measurements. This knowledge would allow the shape and orientation of the relative trajectory to be determined, even though the size of the trajectory cannot be determined.

With this knowledge, one can gain useful information about the relative trajectory such as:

- Whether or not it is drifting
- Whether or not it is centered at the chief
- Whether the radial, in-track, and/or cross-track motion is identically zero
- The phase difference (if any) between the radial/in-track motion and the cross-track motion

A further objective is that this technique should be based on a fundamental understanding of relative motion dynamics and straightforward to apply. The estimation technique demonstrated here is a batch processing routine that iteratively determines the statistical best-fit trajectory for the given angle measurements. This work is based in part on (Reference 6), which was the initial investigation into the problem.

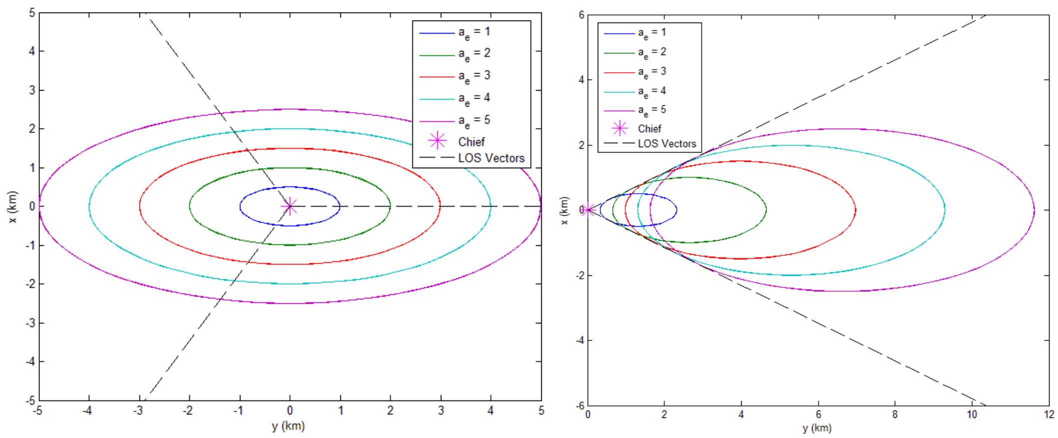

Figure 1. Examples of Families of Relative Orbits with Common LOS Histories (trajectories generated using the Hills-Clohessy-Wiltshire equations[7,8])

INITIAL RELATIVE ORBIT DETERMINATION METHOD

In order to generate an initial guess for a relative navigation technique, an initial orbit determination (IOD) procedure was developed to find the family of relative orbits that correspond to given azimuth and elevation measurements at three different times. If the dynamics are assumed to be linear, the state variables at time t_1 are related to the state variables at time t_0 using a state transition matrix (STM) as follows:

$$\begin{bmatrix}\bar{r}(t_1)\\ \bar{v}(t_1)\end{bmatrix} = \Phi(t_1,t_0)\begin{bmatrix}\bar{r}(t_0)\\ \bar{v}(t_0)\end{bmatrix} \qquad (1)$$

Abbreviating the notation for the position and velocity vectors, the first 3 of these 6 equations may be written as

$$\bar{r}_1 = \Phi_{rr}(t_1, t_0)\bar{r}_0 + \Phi_{rv}(t_1, t_0)\bar{v}_0 \tag{2}$$

where Φrr and Φrv represent 3x3 submatrices of Φ. Similarly, the position vector at time t_2 is related to the position and velocity vector at time t_0 by

$$\bar{r}_2 = \Phi_{rr}(t_2, t_0)\bar{r}_0 + \Phi_{rv}(t_2, t_0)\bar{v}_0 \tag{3}$$

Rewriting $\bar{r}_i$ as $r_i\hat{u}_i$ yields

$$r_1\hat{u}_1 = \Phi_{rr}(t_1, t_0)r_0\hat{u}_0 + \Phi_{rv}(t_1, t_0)\bar{v}_0 \tag{4}$$

$$r_2\hat{u}_2 = \Phi_{rr}(t_2, t_0)r_0\hat{u}_0 + \Phi_{rv}(t_2, t_0)\bar{v}_0 \tag{5}$$

where $\hat{u}_i$ is the LOS vector corresponding to the i^{th} measurement time. These equations may then be rearranged into the following matrix-vector equation:

$$\begin{bmatrix} -\Phi_{rr}(t_1, t_0)\hat{u}_0 & \hat{u}_1 & 0_{3x1} & -\Phi_{rv}(t_1, t_0) \\ -\Phi_{rr}(t_2, t_0)\hat{u}_0 & 0_{3x1} & \hat{u}_2 & -\Phi_{rv}(t_2, t_0) \end{bmatrix} \begin{bmatrix} r_0 \\ r_1 \\ r_2 \\ \bar{v}_0 \end{bmatrix} = 0 \tag{6}$$

or

$$M\bar{\alpha} = 0 \tag{7}$$

Assuming the azimuth and elevation angles (or equivalently, LOS vectors) are known at each measurement time, all elements of M are known and all elements of $\bar{\alpha}$ are unknown. For the case of no measurement noise and no process noise (i.e. assuming the satellites behave according to the dynamics embodied in Φ), M is rank deficient by one due to the LOS ambiguity described above. Thus, there exists a solution for $\bar{\alpha}$, which is the null vector of M (i.e. a basis vector for the one-dimensional null space of M. Solving this null vector (using, for example, a conventional tool such as MATLAB) yields r_0, r_1, r_2, and $\bar{v}_0$. The IOD solution is then obtained by inserting r_0 and $\bar{v}_0$ into the following equation:

$$\bar{x}_{IOD} = \begin{bmatrix} r_0 \hat{u}_0 \\ \bar{v}_0 \end{bmatrix} \; or \; \begin{bmatrix} r_0 u_{0x} \\ r_0 u_{0y} \\ r_0 u_{0z} \\ v_{0x} \\ v_{0y} \\ v_{0z} \end{bmatrix} \tag{8}$$

Since $\bar{\alpha}$ is not unique (i.e. a constant multiple of $\bar{\alpha}$ also solves the equation), neither is $\bar{x}_{POD}$. Therefore, the IOD solution can be standardized as follows:

$$\bar{x}_{IOD}^{\;*} = \begin{bmatrix} 1 \\ \dfrac{u_{0y}}{u_{0x}} \\ \dfrac{u_{0z}}{u_{0x}} \\ \dfrac{v_{0x}}{r_0 u_{0x}} \\ \dfrac{v_{0y}}{r_0 u_{0x}} \\ \dfrac{v_{0z}}{r_0 u_{0x}} \end{bmatrix} \tag{9}$$

Consider the use of the Hills-Clohessy-Wiltshire (HCW) equations[7,8] to model the relative dynamics between the chief and deputy. Key assumptions in the HCW equations are that the two spacecraft are in close proximity, the chief's orbit has zero eccentricity, and only two-body gravitational dynamics are considered. The HCW equations are expressed as

$$\begin{aligned} &\ddot{x} - 2n\,\dot{y} - 3n^2 x = 0 \\ &\ddot{y} + 2n\,\dot{x} = 0 \\ &\ddot{z} + n^2 z = 0 \end{aligned} \tag{10}$$

where x, y, and z are the components of the deputy's position relative to the chief in the local vertical, local horizontal (LVLH) frame. In this frame, the x direction is radial, z is cross-track, and y completes the orthogonal set. For this linear time-invariant system, the STM is a function only of the difference between the initial and final times:

$$\Phi(t_1,t_0)=\Phi(\Delta t)=\begin{bmatrix} 4-3\cos n\Delta t & 0 & 0 & \frac{\sin n\Delta t}{n} & \frac{2(1-\cos n\Delta t)}{n} & 0 \\ 6(\sin n\Delta t - n\Delta t) & 1 & 0 & \frac{2(\cos n\Delta t - 1)}{n} & \frac{4(\sin n\Delta t - 3n\Delta t)}{n} & 0 \\ 0 & 0 & \cos n\Delta t & 0 & 0 & \sin n\Delta t \\ 3n\sin n\Delta t & 0 & 0 & \cos n\Delta t & 2\sin n\Delta t & 0 \\ 6n(\cos n\Delta t - 1) & 0 & 0 & -2\sin n\Delta t & -3+4\cos n\Delta t & 0 \\ 0 & 0 & -n\sin n\Delta t & 0 & 0 & \cos n\Delta t \end{bmatrix} \tag{11}$$

For the case of no measurement noise and no process noise (i.e., the HCW model was used to generate the measurement data), it was shown repeatedly that $\bar{x}_{IOD}$ was exactly equal to the initial state vector from which the measurements were generated (as expected). For cases of nonzero measurement noise and/or process noise, the matrix M is full rank and thus the right-hand side of Eq. (6) cannot be zero. In these cases, the choice of $[r_0 \quad r_1 \quad r_2 \quad \bar{v}_0]^T$ is taken to be the vector corresponding to the smallest singular value of M. This is the vector that minimizes the 2-norm of the right-hand side of Eq. (6). Test results of the IOD method are shown later along with the batch estimator results.

BATCH PROCESSING METHOD

Recall above that when estimating the family of relative orbits corresponding to a given set of angle measurements, there are an infinite number of choices of the true initial basis vector (all of them proportional to one another). Consistent with Eq. (9), in the estimation analysis below, the initial basis vector sought will be the one which has a leading element of 1 or -1 at the epoch time of the estimate:

$$\bar{x}_{0,true} = \begin{bmatrix} \pm 1 \\ y_0 \\ z_0 \\ v_{0x} \\ v_{0y} \\ v_{0z} \end{bmatrix} \tag{12}$$

The measurements are taken to be azimuth and elevation, defined here as

$$\begin{aligned} Az &= ATAN2(z, y) \\ El &= \tan^{-1}\left(\frac{x}{\sqrt{y^2+z^2}}\right) \end{aligned} \tag{13}$$

Note that Az and El can also be defined in terms of LOS vector components:

$$Az = ATAN2(u_z, u_y)$$
$$El = \tan^{-1}\left(\frac{u_x}{\sqrt{u_y^{\,2} + u_z^{\,2}}}\right) \tag{14}$$

The batch estimation process is then a matter of minimizing the RMS error between the true measurements and the measurements as predicted by the estimate. Note that because the leading element of $\bar{x}_{0,true}$ is fixed at 1 or -1, only the 2nd through 6th elements of this vector are to be differentially corrected. The sign of the leading element depends on whether the LOS vector points in the positive or negative x direction. This can be easily determined by examining the measurement data (e.g. the sign of elevation or the sign of u_x). The dynamic model chosen for the estimator was the HCW model detailed in Equations (10)-(11) above. Because HCW dynamics possess a closed-form solution and a known STM, this is essentially a static optimization process (i.e. no numerical propagation is required). So, instead of manually writing code for a batch routine, the standard algorithm "fminunc" in MATLAB was used. The initial guess input to the process is the $\bar{x}_{IOD}$ described in the previous section. The next section describes the test cases that were explored with this technique.

BATCH PROCESSING RESULTS

The batch process was tested with many cases of simulated measurements. In the first set of cases, the measurements were generated between a chief in low Earth orbit and a deputy by propagating the HCW equations for ¼ period of the chief. The azimuth and elevation angles were calculated at each measurement time, and Gaussian noise was added to these to simulate corrupted observation data.

First, measurements were generated using the HCW model (the same model used by the estimator). The following relative motion scenarios were chosen:

- arbitrary motion: $\bar{x}_{0,true}$= [1,4,0.9,-0.2,0.3,-0.4]^T
- stationary 2-D ellipse: $\bar{x}_{0,true}$= [1,0, 0, 0, -2n, 0]^T
- straight-line drift above the chief: $\bar{x}_{0,true}$= [1,0, 0, 0, -1.5n, 0]^T

where n is the mean motion of the chief. Note that the leading element of the basis vector in each scenario is 1, in keeping with the standardization discussion above. Although the units are not crucial since the goal is to find a basis vector for the family of relative orbits (all of which are proportional to one another), for the results shown below, position is taken to be in km and velocity in km/sec. Also, three different levels of noise were chosen (Az/El σ = 1, 0.1, and 0.01 deg). Table 1 annotates the various test cases.

Table 1. Annotation of the Test Cases Involving Measurements Generated from HCW Propagation.

		Arbitrary Relative Motion	2-D Ellipse	Drifting
Noise Level (deg)	1	1	4	7
	0.1	2	5	8
	0.01	3	6	9

Table 2 displays the IOD and batch estimation results for these cases. The RMS residual values represent the RMS error between the "true" azimuth and elevation measurements and those predicted by the estimate. The Xnorm error is the 2-norm of the difference between $\bar{x}_{0,true}$ and the estimate of $\bar{x}_0$. These results show that the IOD method generally produces a reasonable initial guess, while the estimator converges to a solution with significant accuracy. Statistically, the RMS residual error should converge to a value approximately equal to the standard deviation of the measurement noise (for an infinite number of measurements, these two values would be exactly equal). This is in fact the trend in the cases below. Thus, the performance achieved by the estimator for HCW-generated data is quite satisfactory, both in terms of RMS residual error and closeness of the solution to the true epoch state vector.

Table 2. Results for the Test Cases Involving Measurements Generated from HCW Propagation.

Scenario	IOD RMS Residual (deg)	IOD Xnorm Error	RMS Residual for Converged Batch Solution (deg)	Xnorm Error for Converged Batch Solution
1	2.6088	0.33186	0.97497	0.1896
2	0.74934	0.16019	0.095217	0.010023
3	0.054358	0.015315	0.0096282	0.00038282
4	60.187	0.0033419	1.3943	0.003211
5	8.9859	0.0013403	0.10015	0.00040933
6	0.033667	0.00032685	0.033428	0.00032684
7	9.0357	0.0030846	1.0102	0.0034772
8	0.12436	0.0018359	0.098874	0.0018359
9	0.010311	0.000018300	0.01031	0.0000183

The next cases explored involved data generated with standard 2-body propagation. Two relative motion scenarios were chosen, that of a stationary ellipse in 3-D (i.e. including a cross-track component) and a drifting ellipse in 3-D. Table 3 displays the epoch conditions for each scenario in terms of the chief and deputy classical orbit elements, while Table 4 displays the relative state vector at the epoch time calculated from the chief and deputy inertial states and normalized by its leading element. Four different levels of noise were chosen, including zero noise (Az/El σ = 1, 0.1, 0.01, and 0 deg). Table 5 annotates the various test cases.

Table 3. Description of the Two Scenarios Involving Measurements Generated from 2-body Propagation (Chief and Deputy Orbit Elements).

	Stationary 3-D Ellipse		Drifting 3-D Ellipse	
	Chief	Deputy	Chief	Deputy
a (km)	7500	7500	7500	7500.1
e	0	0.0002	0	0.0002
i (deg)	40	40.003	40	40.009
Ω (deg)	30	30	30	30
ω (deg)	12	12	12	12
ν (deg)	1	1	1	1

Table 4. Description of the Two Scenarios Involving Measurements Generated from 2-body Propagation (Epoch Relative State Vector).

	Stationary 3-D Ellipse	Drifting 3-D Ellipse
$x_{0,true}$	-1	-1
$y_{0,true}$	-1.50E-06	-1.45E-05
$z_{0,true}$	0.058889	0.18929
$v_{x0,true}$	1.35E-09	-6.29E-07
$v_{y0,true}$	0.0019441	0.0019788
$v_{z0,true}$	0.00024896	0.00080023

Table 5. Annotation of the Test Cases Involving Measurements Generated from 2-Body Propagation.

		Stationary	Drifting
Noise Level (deg)	1	10	14
	0.1	11	15
	0.01	12	16
	0	13	17

Table 6 displays the IOD and batch estimation results for these cases. These results show an interesting trend. For the two lowest levels of measurement noise ($\sigma = 0$ and 0.01 deg), in both scenarios the RMS residual error converges to a value decidedly larger than σ. This indicates that the error is being driven by process noise, i.e. the fact that the HCW model in the estimator is of lower fidelity than the 2-body model used to generate the measurements. Whereas at measurement noise levels of $\sigma = 0.1$ or larger, the convergence capability of the estimator is being driven by the measurement noise. (One could argue that for case 15, the measurement noise and process noise appear to have an approximately equal effect.) Thus, the performance achieved by the estimator for 2-body-generated data is quite satisfactory, both in terms of RMS residual error and closeness of the solution to the true epoch state vector.

Table 6. Results for the Test Cases Involving Measurements Generated from 2-Body Propagation.

Scenario	Noise Sigma (deg)	IOD RMS Residual (deg)	IOD Xnorm Error	RMS Residual for Converged Batch Solution (deg)	Xnorm Error for Converged Batch Solution
10	1	119.41	0.026925	1.0710	0.0048079
11	0.1	0.33594	0.0011312	0.097706	0.0011088
12	0.01	0.42656	0.00031386	0.068291	4.3841e-05
13	0	0.40933	0.00029997	0.065363	3.8936e-05
14	1	1.3231	0.0092432	0.93641	0.0078048
15	0.1	0.21863	0.00099984	0.16132	0.00099631
16	0.01	0.23245	0.00015977	0.11095	5.0069e-05
17	0	0.22045	0.00014121	0.082245	0.0026812

CONCLUSIONS

The goal of this work was to examine how accurately a basis vector for a family of relative orbit trajectories could be determined from angles-only measurements. An IOD method was introduced that took in angle measurements at three times and produced an initial guess of the basis vector for the batch estimator to correct on. The IOD method was combined with a batch estimator and applied to several candidate scenarios with varying levels of noise added to the data. Generally this approach produced very accurate results. These results show that in angles-only cases where the full relative state is unobservable (i.e. the size or magnitude of the relative orbit cannot be precisely known), other characteristics such as shape, orientation, and drift rate can be determined from the measurements.

Going forward, several tasks to be pursued are:

- Use of higher fidelity dynamics to generate measurements (e.g. non-linear inertial dynamics with high order gravity and perturbations)
- Incorporation of a relative motion model in the estimator that accounts for chief eccentricity
- Inclusion of other solve-for parameters in the relative navigation technique (e.g. environmental parameters)
- Development of different estimator designs (e.g. EKF and/or UKF)

REFERENCES

[1] D. Woffinden and D. Geller, "Observability Criteria for Angles-Only Navigation," AAS Paper 07-402, presented at the AAS/AIAA Astrodynamics Specialist Conference, Mackinac Island, MI, Aug 19-23, 2007.

[2] Y. Qiu, B. Guo, B. Liang, and C. Li, "Hardware-in-Loop Simulation of Autonomous Relative Navigation for Noncooperative Spacecraft," presented at the 2nd International Symposium on Systems and Control in Aerospace and Astronautics, Dec 10-12, 2008.

[3] M. Ilyas, M. Iqbal, J.G. Lee, and C.G. Park, "Extended Kalman Filter Design for Multiple Satellites Formation Flying," presented at the 4th International Conference on Emerging Technologies, Oct 18-19. 2008.

[4] D.C. Maessen and E. Gill, "Relative State Estimation and Observability for Formation Flying Satellites in the Presence Of Sensor Noise," presented at the 6th International Workshop on Satellite Constellation and Formation Flying, Taipei, Taiwan, November 1-3, 2010.

[5] J. Tombasco, "Orbit Estimation of Geosynchronous Objects Via Ground-Based and Space-Based Optical Tracking," Ph.D. Dissertation, University of Colorado, 2011, pp. 98-112.

[6] J. Schmidt and T.A. Lovell, "Estimating Geometric Aspects of Relative Satellite Motion Using Angles-Only Measurements," AIAA Paper 2008-6604, presented at the AAS/AIAA Astrodynamics Specialist Conference, Honolulu, HI, Aug 18-21, 2008.

[7] G.W. Hill, "Researches in the Lunar Theory," *American Journal of Mathematics,* Volume 1, 1878, pp. 5-26.

[8] W.H. Clohessy and R.S. Wiltshire, "Terminal Guidance System for Satellite Rendezvous", *Journal of the Aerospace Sciences,* Vol. 27, No. 9, 1960, pp. 653-658.